



# Functionalized polypyrrole nanotube arrays as electrochemical biosensor for the determination of copper ions

Meng Lin<sup>a,b</sup>, Xiaoke Hu<sup>a,b</sup>, Zhaohu Ma<sup>c</sup>, Lingxin Chen<sup>a,b,\*</sup>

<sup>a</sup> Key Laboratory of Coastal Zone Environmental Processes, Yantai Institute of Coastal Zone Research (YIC), Chinese Academy of Sciences (CAS), Yantai 264003, PR China

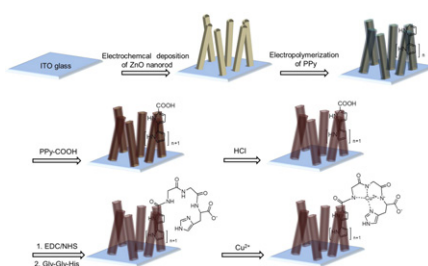
<sup>b</sup> Shandong Provincial Key Laboratory of Coastal Zone Environmental Processes, YICCAS, Yantai 264003, PR China

<sup>c</sup> Marine Environmental Monitoring and Forecasting Center of Yantai, Yantai 264003, PR China

## HIGHLIGHTS

- ▶ PPy nanotube arrays were electropolymerized using ZnO nanowire arrays as templates.
- ▶ PPy nanotube arrays were anchored onto ITO glass without any chemical linker.
- ▶ Using SWV, the biosensor was found to be highly sensitive and selective to  $\text{Cu}^{2+}$ .
- ▶ The biosensor was successfully applied for the determination of  $\text{Cu}^{2+}$  in drinking water.

## GRAPHICAL ABSTRACT



## ARTICLE INFO

### Article history:

Received 24 June 2012

Received in revised form 14 August 2012

Accepted 16 August 2012

Available online 23 August 2012

### Keywords:

Electrochemical biosensor  
Conducting polymer  
Polypyrrole nanotube arrays  
Zinc oxide nanowire arrays  
Copper ions

## ABSTRACT

A novel electrochemical biosensor based on functionalized polypyrrole (PPy) nanotube arrays modified with a tripeptide (Gly-Gly-His) proved to be highly effective for electrochemical analysis of copper ions ( $\text{Cu}^{2+}$ ). The vertically oriented PPy nanotube arrays were electropolymerized by using modified zinc oxide (ZnO) nanowire arrays as templates which were electrodeposited on indium–tin oxide (ITO) coated glass substrates. The electrodes were functionalized by appending pyrrole- $\alpha$ -carboxylic acid onto the surface of polypyrrole nanotube arrays by electrochemical polymerization. The carboxylic groups of the polymer were covalently coupled with the amine groups of the tripeptide, and its structural features were confirmed by attenuated total reflection infrared (ATR-IR) spectroscopy. The tripeptide modified PPy nanotube arrays electrode was used for the electrochemical analysis of various trace copper ions by square wave voltammetry. The electrode was found to be highly sensitive and selective to  $\text{Cu}^{2+}$  in the range of 0.1–30  $\mu\text{M}$ . Furthermore, the developed biosensor exhibited a high stability and reproducibility, despite the repeated use of the biosensor electrode.

© 2012 Elsevier B.V. All rights reserved.

## 1. Introduction

Conducting polymer (CP) nanomaterials are of great importance in a wide application areas concerning with electronics, optoelectronics, energy storage and chemical/biological sensing [1]. Due to its environmental stability, good biocompatibility and high electronic conductivity, CP nanomaterials have attracted great attention in the fabrication of chemical and biosensors [2]. The strategies for CP nanomaterials to obtain highly sensitive and specific responses focus on the integration with various

\* Corresponding author at: Key Laboratory of Coastal Zone Environmental Processes, Yantai Institute of Coastal Zone Research, Chinese Academy of Sciences, Chunhui Rd 17, Laishan District, Yantai 264003, PR China. Tel.: +86 535 2109130; fax: +86 535 2109130.

E-mail address: [lxchen@yic.ac.cn](mailto:lxchen@yic.ac.cn) (L. Chen).

micro-analytical systems and coupling with chemical/biological species [3]. Especially, the functionalized CP nanowires (NW) and nanotubes (NT) are predicted to be excellent sensing materials relating with their features of high surface areas, porous structure, abundant surface functionalities, and sensitive electron transduction [4]. Among the CP nanomaterials, PPy nanomaterials are very attractive substrates for immobilization of biomaterials, rendering their wide utilization for the design and construction of various biosensors harnessing immobilized enzymes, and covalently attached ligands or specific biological species [5–8].

Various methods, such as hard [9] and soft templating [10], interfacial polymerization [11], and seed/oligomer-assisted synthesis [12], have been developed to prepare CP nanomaterials, but most CP nanomaterials suffer from insufficient adhesion to the electrode substrates. Those CP nanomaterials have been used to detect the analytes predominantly present in the gas phase. To overcome these limitations, several strategies have been proposed. Lee and co-workers reported a copper ions ( $\text{Cu}^{2+}$ ) biosensor based on an overoxidized PPy NW layer. The overoxidized PPy NW layer was formed by one step pyrrole electropolymerization in the presence of sodium carbonate [5]. A biosensor based on enzyme functionalized poly(pyrrole-3-carboxylic acid) NTs which were immobilized onto a microelectrode substrate via covalent linkages was developed by Jang and co-workers [3]. However, to the best of our knowledge, no electrochemical biosensors have been reported based on peptide modified PPy NT arrays electrodes.

Controlling the orientation of CP nanomaterials during polymerization is critically important [13]. Current research trends mainly focus on the investigation of CP nanomaterial arrays, because they exhibit a unique combination of morphology and intrinsic properties, such as high surface to volume ratio, fast oxidation/reduction kinetic and electrical conductivity [14]. Hard-template assisted synthesis has been a common approach to produce ordered CPs nanomaterial arrays. The generally used two types of templates are track-etched polymeric membranes and porous anodic aluminum oxide (AAO) membranes [15,16]. The templates especially attracted extensive interest due to their uniform pore diameters and ordered porous distribution [17]. However, upon removal of the templates the CP nanoarrays collapse onto the substrate, losing their orientation. Thus, it is not easy to obtain the CP nanoarrays standing vertically on a substrate after removing the templates [18,19]. On the other hand, the high costs of template and the complex handling processes also limit the applications using CPs nanomaterial arrays [20]. Recently, studies on CP nanomaterial arrays without using templates have attracted great attentions. Dilute chemical oxidative polymerization has been introduced to synthesize polyaniline nanofiber arrays [21]. Li et al. reported a one-step electropolymerization strategy to synthesize polypyrrole (PPy) nanofiber arrays in a biphasic electrochemical system [1]. Oriented PPy NW arrays formed just using one-step electropolymerization by electrogenerating PPy in the presence of jointly non-acidic and weak-acidic anions without any templates [22]. Nonetheless, these methods are time-consuming, and the sizes of CP nanomaterial arrays are still difficult to control [23].

Herein, we first report a novel electrochemical biosensor harnessing the tripeptide Gly-Gly-His (GGH) covalently attached to PPy NT arrays on an indium–tin oxide (ITO) coated glass electrode for determination of  $\text{Cu}^{2+}$  with the lower concentration. PPy NT arrays were electropolymerized with controlled dimensions and morphologies by using a zinc oxide (ZnO) NW arrays as a versatile template. The carboxyl group of the polymer was modified to accommodate tripeptide molecules for  $\text{Cu}^{2+}$  capture. In the present study, the GGH modified PPy NT arrays biosensor proved its capability to determine the concentration of  $\text{Cu}^{2+}$  in the range of 0.1–30  $\mu\text{M}$ .

## 2. Experimental

### 2.1. Materials and characterization

Pyrrole (98%), N-hydroxysuccinimide (NHS), 1-ethyl-3-(3-dimethylamino propyl)-carbodiimide hydrochloride (EDC), copper(II) chloride hydrate, potassium chloride (KCl, 99.5%), zinc chloride ( $\text{ZnCl}_2$ ), lithium perchlorate ( $\text{LiClO}_4$ ), methylene chloride ( $\text{CH}_2\text{Cl}_2$ ), and acetonitrile (ACN) were purchased from Aladdin Chemistry Co. Ltd. (Shanghai, China). GGH, pyrrole- $\alpha$ -carboxylic acid (99%, Py- $\alpha$ -COOH) and tetrabutylammonium hexafluorophosphate were obtained from Sigma–Aldrich. 2-(N-morpholino)ethanesulfonic acid (MES) hydrate, ammonium acetate, sodium hydroxide, and sodium chloride were used for buffer solutions. All chemicals were of reagent grade and used without further purification.

All solutions were freshly prepared using freshly de-ionized water (18.2 M $\Omega$  cm, Pall Corp., USA). 100 mM MES (pH 6.8) was used in further modification steps. Stock solution of copper ions (5 mM) was prepared in 50 mM ammonium acetate buffer (pH 7.0) and diluted to give various concentrations of copper ions.

Surface morphology of the electrodes was examined by scanning electron microscopy (SEM, Hitachi S-4800, Japan). Attenuated total reflection infrared (ATR-IR) spectra were obtained by infrared spectrophotometry (Thermo Scientific Nicolet iS 10), using an ATR platform by pressing the solid electrodes onto the GaAs crystal. Cyclic voltammetry of the electrode was conducted in a copper ion-free buffer (50 mM ammonium acetate, 50 mM NaCl, pH 7.0) at a sweep rate of 100 mVs<sup>-1</sup>. All electrochemical analysis was performed in a conventional three-electrode cell comprising the modified electrode as a working electrode, a platinum plate as a counter electrode, and a saturated calomel electrode (SCE) in saturated KCl solution as a reference electrode using a CHI 660C electrochemical workstation (Chenhua Instruments, Shanghai, China).

### 2.2. Preparation of ZnO NW array electrodes

ZnO NW arrays were prepared by electrodeposition process according to the previous literature [24]. Prior to the electrodeposition, the indium–tin oxide (ITO) coated glass (1 cm  $\times$  5 cm) was cleaned in an ultrasonic bath for 20 min each in acetone, ethanol, and distilled water, respectively. The electrolyte was a  $1 \times 10^{-3}$  M  $\text{ZnCl}_2$  and 2 M KCl ultrapure aqueous solution, saturated with bubbling oxygen. The applied potential was operated at  $-1$  V versus SCE for 90 min and the deposition was conducted at a temperature of 80 °C.

### 2.3. Preparation of PPy-COOH NT array electrodes

Carboxyl end-capped PPy (PPy-COOH) NT arrays were electropolymerized in three steps by using the ZnO NW arrays as templates. The PPy was electropolymerized in a methylene chloride solution containing 0.01 M pyrrole and 0.05 M tetrabutylammonium hexafluorophosphate by chronoamperometry at 1.20 V for 90 s. After a thorough rinse with fresh ethanol, the ZnO/PPy hybrid nanoarray electrode was transferred into a cell to create ZnO/PPy-COOH hybrid nanoarrays, 0.01 M Py- $\alpha$ -COOH in ACN containing 0.05 M  $\text{LiClO}_4$  as supporting electrolyte. A voltage at 2.0 V was applied for 15 min to ensure the  $\alpha$ -terminus C–C coupling between PPy and Py- $\alpha$ -COOH [25]. Then, the ZnO/PPy-COOH hybrid nanoarray electrode was immersed in fresh ethanol to eliminate the residual monomer. Subsequently, the electrode was immersed in 1 M HCl solution for a few seconds to remove ZnO from the hybrid nanoarrays. The obtained PPy-COOH NT arrays electrode was rinsed with de-ionized water and stored in 50 mM ammonium acetate buffer (pH 7.0).

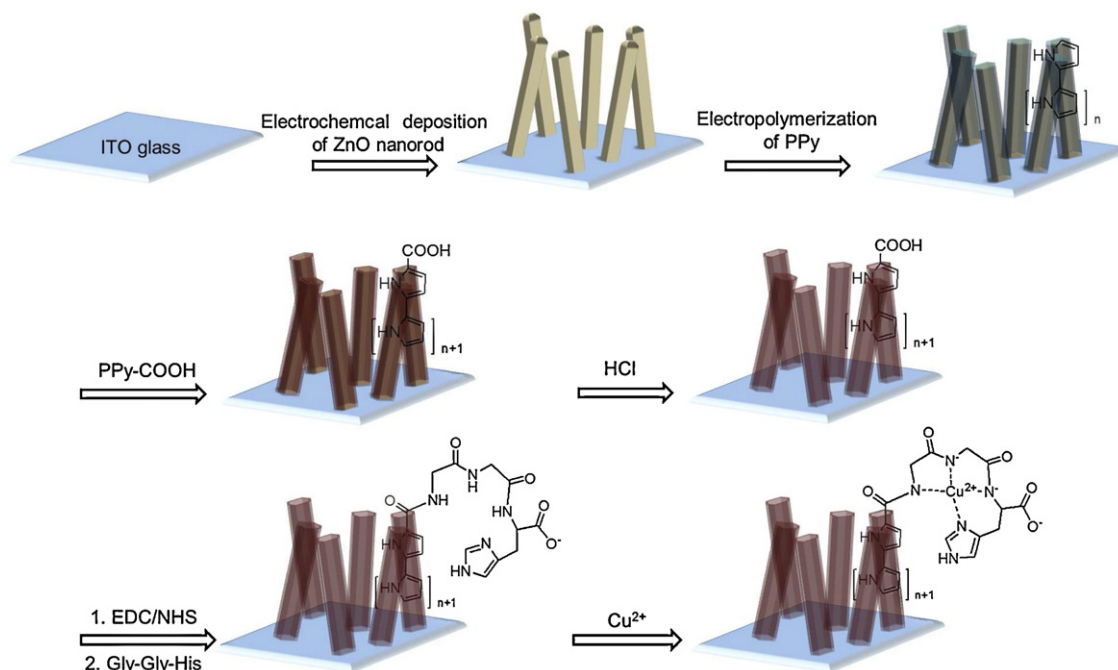


Fig. 1. A schematic of the GGH modified PPy NT arrays electrode synthesis and its putative complexation with Cu<sup>2+</sup>.

#### 2.4. Modification of PPy-COOH NT array electrode with GGH tripeptide

The modification of PPy-COOH NT array electrode with tripeptide (GGH) was performed as reported elsewhere [26,27]. The carboxyl terminal groups of the PPy-COOH were activated in a solution of 50 mM EDC/50 mM NHS in 100 mM MES (pH 6.8) for 3 h. After a thorough rinse with 25 mM MES buffer, the polymer electrode was reacted overnight with GGH (3 mg mL<sup>-1</sup>) in 100 mM MES buffer to form the peptide conjugated PPy-COOH (PPy-GGH) electrode. The modified electrode was rinsed thoroughly with 25 mM MES buffer and stored at room temperature in 50 mM ammonium acetate buffer (pH 7.0) prior to use.

#### 2.5. Metal ion sensing

The PPy-GGH nanoarray electrode was immersed in 20 mL of 50 mM aqueous ammonium acetate buffer solution (pH 7.0) at various concentrations of copper ions for 10 min and washed with copper-free ammonium acetate buffer. The bound metal ions on the PPy-GGH nanoarray electrode were reduced at -1.0 V for 60 s, and the electrochemical response was measured by square wave voltammetry (SWV) using a frequency of 15 Hz, an amplitude of 25 mA, and a step voltage of 4 mV. After each SWV measurement, the electrode was rinsed with ammonium acetate buffer, placed in 0.1 M ethylenediaminetetraacetic acid (EDTA) solution for regeneration, rinsed with acetate buffer, reduced and measured by SWV in a fresh ammonium acetate buffer to ensure complete stripping of all metal ions.

### 3. Results and discussion

#### 3.1. Preparation and characterization of PPy-GGH nanoarray electrodes

Fig. 1 illustrates the steps involved in the electrodeposition of ZnO NW arrays, electropolymerization and preparation of PPy-COOH NT arrays and the GGH tripeptide modification processes. ZnO NW arrays were electrodeposited on the surface of ITO glass

substrate, and the ZnO NW arrays were used as a template for preparation of PPy NT arrays. A layer of PPy was covered around the ZnO NW arrays by electropolymerization, and then a monolayered PPy-COOH was formed through the coupling reaction between the  $\alpha$ -terminus of PPy and the  $\alpha$ -end of Py- $\alpha$ -COOH [28]. The ZnO NW array template was removed by using HCl solution to obtain the PPy-COOH NT arrays. Subsequently, the monolayer carboxyl terminal groups of the PPy-COOH NT arrays were activated and modified with GGH tripeptide for Cu<sup>2+</sup> electrochemical detection. The use of oriented ZnO NW arrays as templates has been proposed as an alternative to AAO template because of the easily scalable deposition techniques and its facile removal through etching [19,29]. Moreover, the aligned nanostructures of the functional materials can be found to be advantageous for applications [1,23].

##### 3.1.1. Surface morphology

The structures of the ZnO NW arrays and PPy NT arrays were investigated by SEM analysis. According to the literature [30], low concentration of Zn<sup>2+</sup> precursor is the key for growing ZnO NW, and high concentration of Cl<sup>-</sup> also favors the growth of ZnO NW [31]. The inset of Fig. 2a is a low-magnified SEM image of ZnO NW arrays, showing the ZnO NW arrays grown on ITO glass substrate, which have a random orientation. It can be seen that the ZnO NWs are aligned nearly perpendicular to the substrate. The ZnO NWs range from 380 nm to 410 nm in diameter and around 1.6  $\mu$ m in length. The top surface of the ZnO NWs becomes thinner and has a slightly hexagonal facet, which is in good agreement with the morphology reported by Tena-Zaera and co-workers [24]. In order to obtain PPy-COOH NT arrays, PPy was firstly electropolymerized onto the surface of the ZnO NWs, achieving the ZnO/PPy hybrid arrays. The second step toward PPy-COOH NT arrays involves the electropolymerization of Py- $\alpha$ -COOH onto the ZnO/PPy hybrid arrays. Fig. 2b and c shows the morphology of PPy and PPy-COOH NT arrays after selectively removing the ZnO template. The free standing PPy and PPy-COOH NT arrays on the surface of ITO glass were obtained. Obviously, the SEM images reveal that both PPy and PPy-COOH NT arrays represent homogenous nanostructures. The walls thickness of the PPy NT arrays is ca. 60–70 nm, and the carboxylation of PPy



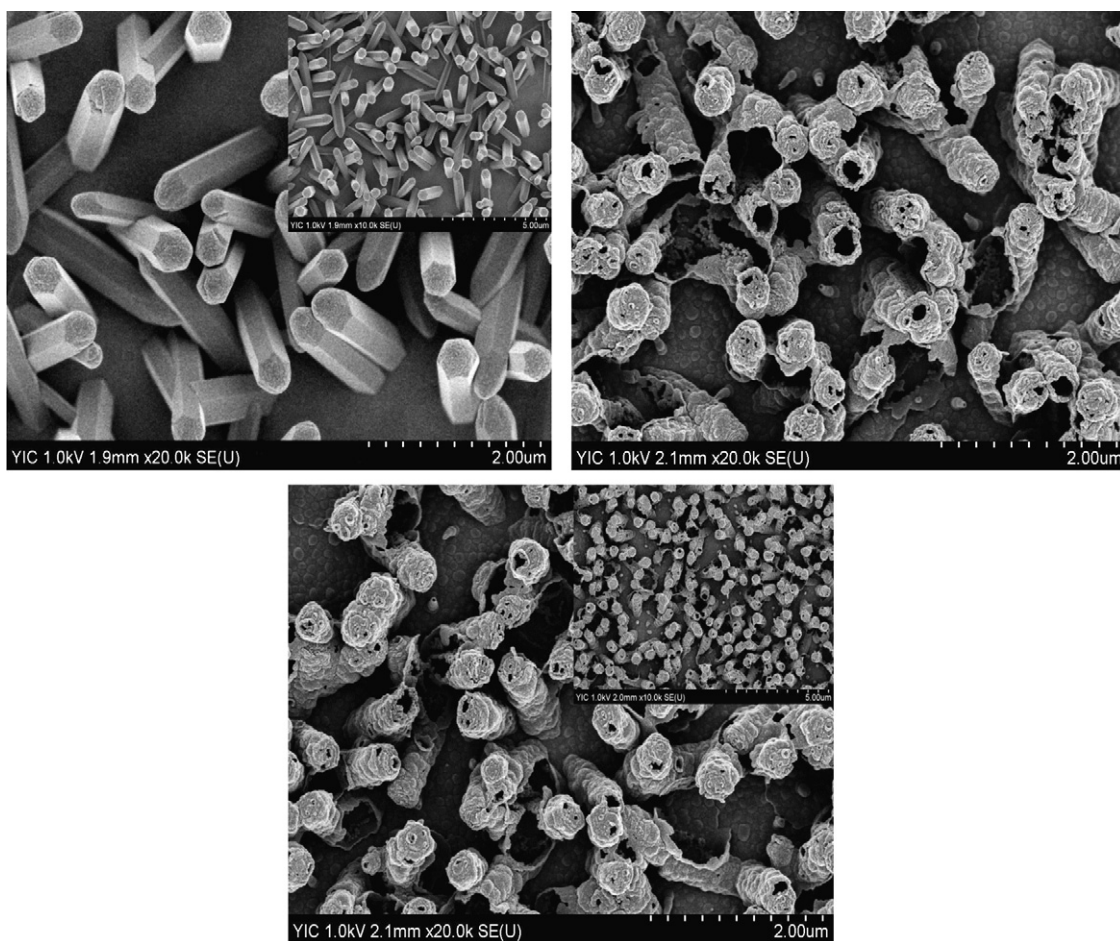


Fig. 2. SEM images of (a) ZnO NW arrays, (b) PPy NT arrays, and (c) PPy-COOH NT arrays.

NT arrays to give rise to PPy-COOH NT arrays rarely affects the morphological features since neither the overall NT structure nor the apparent diameter of the NT changed [5]. The morphology of the PPy NT arrays is of cauliflower shape, similar as that of the final PPy-COOH NT arrays. It is worth mentioning that the overall structure of the PPy-COOH is mostly governed by the PPy underlayer, and there should be only slight changes on the carboxyl end-capped surface [25]. The cauliflower surface structure of the PPy-COOH NT arrays could allow a large surface area for efficient binding of  $\text{Cu}^{2+}$  ions.

### 3.1.2. ATR-IR spectroscopy

The ATR-IR spectrum of PPy NT arrays is displayed in Fig. 3a. The band is observed at  $1041\text{ cm}^{-1}$ , corresponding to the N–H in-plane deformation vibration of pyrrole rings. The band assigned to the C–H in-plane stretching vibration appears at  $1306\text{ cm}^{-1}$  [32]. The bands at  $1462$  and  $1167\text{ cm}^{-1}$  can be attributed to the C–C ring and C–N stretching vibrations, respectively [33]. The C=C stretching vibration of pyrrole ring in PPy can be found at  $1540\text{ cm}^{-1}$  [34]. The spectrum of PPy-COOH NT arrays (Fig. 3b) exhibits a characteristic band at  $1709\text{ cm}^{-1}$ , which attributed to the monolayer of carboxylic acid groups, accounting for successful incorporation of the carboxyl group from Py- $\alpha$ -COOH to the surface of PPy NT arrays [35]. The PPy NT arrays can be further overoxidized at high positive potential (i.e. 2.0 V). Oxygen-containing groups were introduced as a result of overoxidation, along with the loss of the cationic charge on the pyrrole nitrogen [36]. As shown in Fig. 3b, the peak at about  $1625\text{ cm}^{-1}$  is attributed to the C=O stretching, indicating that the overoxidation process occurred at the pyrrole rings and carbonyl groups were introduced in the polymer backbone after

overoxidation [37]. The modification of the tripeptide GGH on the PPy-COOH NT arrays revealed one carboxylic acid group of PPy-COOH NTs replaced by one tripeptide molecule (Fig. 1). In the ATR-IR spectrum of PPy-GGH nanoarrays (Fig. 3c), the band at  $1708\text{ cm}^{-1}$  increased attributed to the C=O groups introduced by the tripeptide GGH, the result is in good agreement with the predicted surface structure of PPy-COOH functionalized with GGH through an amide bond.

### 3.1.3. Cyclic voltammetry

The electrochemical behaviors of the PPy NT arrays and PPy-COOH NT arrays were investigated by cyclic voltammetry in a copper ion-free buffer (50 mM ammonium acetate, 50 mM NaCl, pH 7.0) at a sweep rate of  $100\text{ mV s}^{-1}$  (Fig. 4a). The cyclic voltammogram of the PPy NT arrays is depicted in Fig. 4a (dash line), a slight coupling anodic and cathodic peaks are observed close to  $+0.62$  and  $-0.36\text{ V}$ , respectively. The PPy NT arrays are subjected to a reproducible redox process, which is the well known characteristic of an electrochemical system employing the pyrrole series [38]. The PPy NT arrays were overoxidized by applying the potential of 2 V during the formation process of PPy-COOH NT arrays. Due to the irreversible degradation process of the PPy NT arrays by overoxidation (solid line, Fig. 4a), the peak current of the PPy-COOH NT arrays decreases distinctly after incorporation of Py- $\alpha$ -COOH onto the surface of PPy NT arrays [36].

Fig. 4b shows the cyclic voltammograms recorded for the PPy-GGH nanoarray electrode (solid line) and the PPy-GGH nanoarray electrode with  $\text{Cu}^{2+}$  captured in copper solution (dash line) for 10 min. The electrochemical response for the bare PPy-GGH

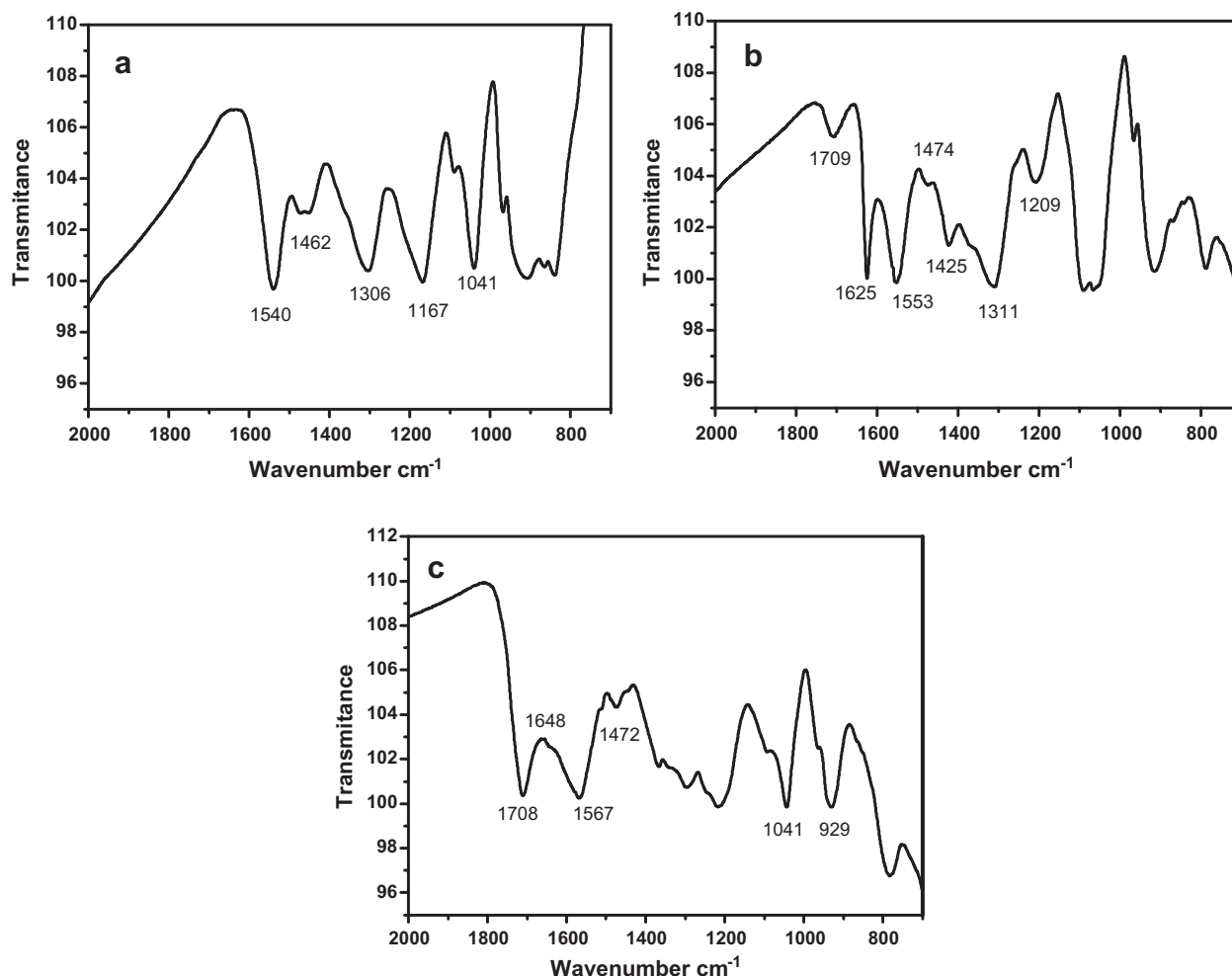


Fig. 3. ATR-IR spectra for the (a) PPy NT arrays electrode, (b) PPy-COOH NT arrays electrode, and (c) PPy-GGH nanoarray electrode.

nanoarrays shows no obvious electrochemical response between  $-0.6$  and  $+0.6$  V. For the  $\text{Cu}^{2+}$  captured electrode, a few apparent redox peaks appeared at  $-0.148$  V and  $-0.168$  V. These peaks are clearly attributed to the redox reaction of  $\text{Cu}^0/\text{Cu}^{2+}$  [26,27], confirming the attachment of GGH tripeptide to the PPy-COOH NT arrays electrode.

### 3.2. Electrochemical performance of PPy-GGH nanoarray electrode

Square wave stripping voltammetry analysis has higher sensitivity than other electrochemical techniques in the determination of trace metal ions [39]. The stripping techniques comprise of two steps. The first step is the accumulation of copper ions by PPy-GGH nanoarrays, and the second step involves in stripping. The stripping method using chemically modified electrode has higher selectivity due to the selective affinity of the tripeptide GGH modifier to capture  $\text{Cu}^{2+}$  [26,40]. In addition, its small size is ideal for locating the peptide probe to the transducer in close proximity which facilitating the PPy-GGH nanoarray electrode to detect  $\text{Cu}^{2+}$  in a selective manner [5].

We investigated the SWV response of the PPy-GGH nanoarray electrodes between  $-0.4$  and  $+0.3$  V. The SWV peaks originating from PPy-GGH nanoarray electrodes are shown in Fig. 5. Following the capture step, the modified electrode was transferred into a copper ion-free buffer (50 mM ammonium acetate, 50 mM NaCl, pH 7.0) for detection of  $\text{Cu}^{2+}$  where the captured metal ions on the

electrode surface were reduced before recording the stripping current using SWV [41]. The overoxidized PPy could avoid its large background current that may hinder an accurate determination of a SWV peak current arising from oxidation of  $\text{Cu}^0$  in the polymer matrix [5]. As illustrated in Fig. 5, SWV reveals a distinctive peak at  $-168$  mV, associating with the oxidation of  $\text{Cu}^0/\text{Cu}^{2+}$  on a PPy-GGH nanoarray electrode [41]. The peak current from SWV is proportional to the amount of copper ions bound to the PPy-GGH nanoarray electrode surface. The calibration curve (Fig. 5 insert) shows a linear increase in current density depending on the  $\text{Cu}^{2+}$  concentration from  $0.1$  to  $30 \mu\text{M}$  ( $R^2 = 0.9902$ ), illustrating a high sensitivity of the PPy-GGH nanoarray electrode to  $\text{Cu}^{2+}$ . The detection limit, calculated as the blank signal plus three times the blank standard deviation, is  $46 \text{ nM}$ . From Fig. S1 (supplementary material), it is clearly observed that a small oxidation background current peak from the PPy-GGH was at  $-55$  mV, and the magnitude of current is comparable to that from a significantly lower  $\text{Cu}^{2+}$  concentration (i.e.  $0.5 \mu\text{M}$ ) [5]. However, each Cu oxidation peak emerged at  $-168$  mV for the PPy-GGH nanoarray electrode is distinctive from the background in a concentration dependent manner, rendering a clear determination of the peak current for each SWV curve. Therefore, the background current peak only can be recognized at low concentration, and the small oxidation peak could be a negligible background current from PPy-GGH nanoarray electrode at high concentration of  $\text{Cu}^{2+}$ . The electrochemical analytical parameters of some reported CPs based electrodes using different modification approaches for  $\text{Cu}^{2+}$  sensing were

**Table 1**  
Electrochemical analysis of various conducting polymer modified electrodes for  $\text{Cu}^{2+}$  determination.

Conducting polymer	Electrochemical technique	Detection range ( $\text{Cu}^{2+}$ , $\mu\text{M}$ )	Selectivity	Ref.
PPy nanowire	SWV	0.02–0.3	$\text{Cu}^{2+}$	[5]
PT <sup>a</sup> film	SWV	0.1–10	$\text{Pb}^{2+}$ , $\text{Cu}^{2+}$	[27]
PPy film	SWV		$\text{Pb}^{2+}$ , $\text{Cu}^{2+}$	[41]
PT film	SWV	0.005–10	$\text{Pb}^{2+}$ , $\text{Cu}^{2+}$ , $\text{Hg}^{2+}$	[42]
PPy nanoarray	SWV	0.1–30	$\text{Cu}^{2+}$	This work

<sup>a</sup> Polythiophene.

summarized in Table 1 and compared with the PPy-GGH nanoarrays electrode obtained in this study.

### 3.3. Selectivity and regeneration of the PPy-GGH nanoarray electrodes

The selectivity of the PPy-GGH nanoarray electrode was investigated in the presence of common metal ion interferences, such as  $\text{Ni}^{2+}$ ,  $\text{Pb}^{2+}$  and  $\text{Co}^{2+}$ . The PPy-GGH nanoarray electrode has a preferential high affinity toward  $\text{Cu}^{2+}$  and is nearly insensitive to  $\text{Ni}^{2+}$ ,  $\text{Pb}^{2+}$  and  $\text{Co}^{2+}$  (Fig. S2 in supplementary material), which is in good agreement with the previous literatures [5,26].

The reproducibility of the biosensor was found to be excellent as evidenced by a relative standard deviation of 4.5% from five separate measurements. After each measurement, the regeneration of electrodes was performed by immersing the used electrode in

100 mM EDTA aqueous solution for 10 min. There were only 3–4% decreases in peak currents compared to use the fresh prepared tripeptide modified electrode, indicating that the regenerated electrode can be used for repeated  $\text{Cu}^{2+}$  detection in a reproducible manner. Each regenerated electrode was confirmed to be used for determination of copper ions without significant loss of sensitivity for more than 1 month.

### 3.4. Application

The performance of the PPy-GGH nanoarray electrode was investigated by the determination of  $\text{Cu}^{2+}$  in drinking water. The drinking water containing various ions ( $\text{Sr}^{2+}$ ,  $\text{K}^+$ ,  $\text{Na}^+$ ,  $\text{Mg}^{2+}$ ,  $\text{SO}_4^{2-}$ ,  $\text{Cl}^-$ , etc.) was analyzed without pretreatment. For practical

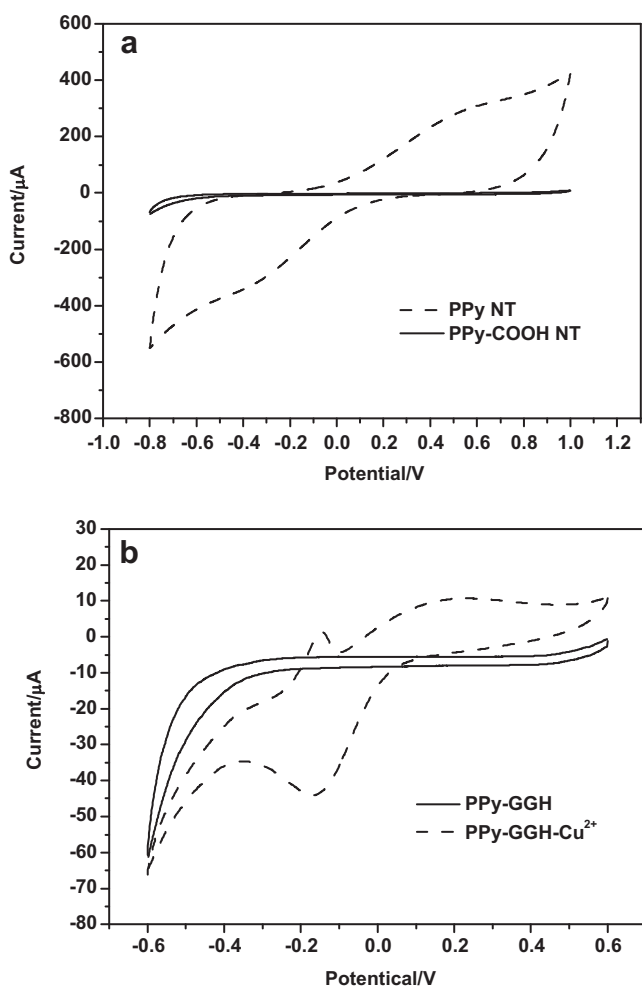


**Fig. 4.** Cyclic voltammetry of PPy-GGH nanoarray electrode (solid line) and PPy-GGH nanoarray electrode with  $\text{Cu}^{2+}$  captured (dash line).

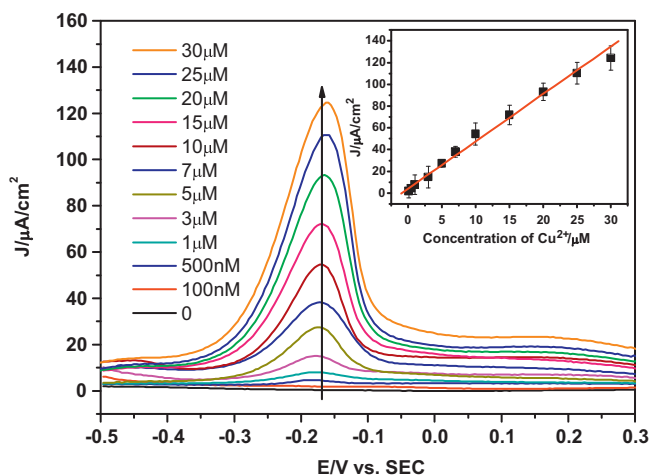


**Fig. 5.** SWV curves for dissolution of  $\text{Cu}^{2+}$  captured by GGH modified PPy-COOH NT arrays electrode in the range of 0.1–30  $\mu\text{M}$   $\text{Cu}^{2+}$ .

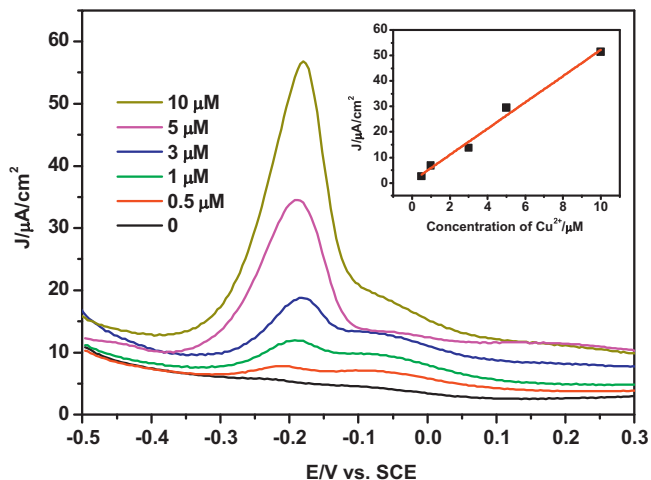


**Fig. 6.** SWV curves of PPy-GGH nanoarray electrode to the addition of various concentrations of  $\text{Cu}^{2+}$  (0, 0.5, 1.0, 3.0, 5.0, and 10  $\mu\text{M}$ ) in the drinking water.

purposes, the drinking water was spiked with standard  $\text{Cu}^{2+}$  solution, in order to simulate the  $\text{Cu}^{2+}$  contaminated water. Fig. 6 shows the SWV responses of the drinking water spiked with 0, 0.5, 1.0, 3.0, 5.0, and 10  $\mu\text{M}$   $\text{Cu}^{2+}$ . It can be seen that the peak current of  $\text{Cu}^{2+}$  increases linearly with increasing the spiked concentration of  $\text{Cu}^{2+}$  in the drinking water. In the case of the original drinking water, there is no clear electrochemical response. The inset shows that a linear relationship ( $R^2=0.9859$ ) obtained when the current response is plotted against the  $\text{Cu}^{2+}$  concentration. This result demonstrates the developed PPy-GGH nanoarray electrode was potentially applicable for the determination of  $\text{Cu}^{2+}$  in drinking and environmental water samples.

#### 4. Conclusions

A novel electrochemical biosensor based on carboxyl end-capped PPy NT array electrode modified with the tripeptide GGH was constructed. ZnO NW arrays were used as templates for the electropolymerization of PPy NT arrays. The modification steps of PPy NT arrays with GGH were characterized by ATR-IR. The electrochemical performance of the PPy-GGH nanoarray electrode was demonstrated by implementing square wave voltammetry for  $\text{Cu}^{2+}$  detection. The PPy-GGH nanoarray electrode reveals highly sensitive to detect  $\text{Cu}^{2+}$  in the range of 0.1–30  $\mu\text{M}$  with a detection limit of 46 nM. The PPy-GGH nanoarray electrodes are also stable and can be reused by a simple wash in EDTA solution for regeneration. This simple strategy provides a new route to fabricate electrochemical sensors based on conducting polymer nanoarrays. Controlling the orientation of PPy NT arrays during growth facilitates the subsequent fabrication processes and develops the design space for novel applications.

#### Acknowledgements

This work was financially supported by the Scientific Research Foundation for the Returned Overseas Chinese Scholars, State Education Ministry, the National Natural Science Foundation of China (21275158), the Science and Technology Development Plan of Yantai (2005124), the Innovation Projects of the Chinese Academy of Sciences (KZCX2-EW-206), and the 100 Talents Program of the Chinese Academy of Sciences.

#### Appendix A. Supplementary data

Supplementary data associated with this article can be found, in the online version, at <http://dx.doi.org/10.1016/j.aca.2012.08.017>.

#### References

- [1] M. Li, Z.X. Wei, L. Jiang, *J. Mater. Chem.* 18 (2008) 2276–2280.
- [2] L. Liu, N. Jia, Q. Zhou, M. Yan, Z. Jiang, *Mater. Sci. Eng. C* 27 (2007) 57–60.
- [3] H. Yoon, J. Jang, *Adv. Funct. Mater.* 19 (2009) 1567–1576.
- [4] S. Ko, J. Jang, *Biomacromolecules* 8 (2007) 1400–1403.
- [5] M. Lin, M. Cho, W.S. Choe, J.B. Yoo, Y. Lee, *Biosens. Bioelectron.* 26 (2010) 940–945.
- [6] T. Lee, Y.B. Shim, S.C. Shin, *Synth. Met.* 126 (2002) 105–110.
- [7] V. Laurinavicius, J. Razumienė, B. Kurtinaitienė, I. Lapenaite, I. Bachmatova, L. Marcinkeviciene, R. Meskys, A. Ramanavicius, *Bioelectrochemistry* 55 (2002) 29–32.
- [8] A. Ramanaviciene, A. Ramanavicius, *Biosens. Bioelectron.* 20 (2004) 1076–1082.
- [9] Y. Xia, P. Yang, Y. Sun, Y. Wu, B. Mayers, B. Gates, Y. Yin, F. Kim, H. Yan, *Adv. Mater.* 15 (2003) 353–389.
- [10] M. Goren, R.B. Lennox, *Nano Lett.* 1 (2001) 735–738.
- [11] J.X. Huang, R.B. Kaner, *Chem. Commun.* (2006) 367–376.
- [12] X.Y. Zhang, S.K. Manohar, *J. Am. Chem. Soc.* 127 (2005) 14156–14157.
- [13] M.R. Abidian, D.C. Martin, *Biomaterials* 29 (2008) 1273–1283.
- [14] S.I. Cho, S.B. Lee, *Acc. Chem. Res.* 41 (2008) 699–707.
- [15] C.R. Martin, *Science* 266 (1994) 1961–1966.
- [16] M. Nishizawa, V.P. Menon, C.R. Martin, *Science* 268 (1995) 700–705.
- [17] R. Liu, S.B. Lee, *J. Am. Chem. Soc.* 130 (2008) 2942–2943.
- [18] J.I. Lee, S.H. Cho, S.-M. Park, J.K. Kim, J.K. Kim, J.-W. Yu, Y.C. Kim, T.P. Russell, *Nano Lett.* 8 (2008) 2315–2320.
- [19] M. Döbbelin, R. Tena-Zaera, P.M. Carrasco, J.R. Sarasua, G. Cabanero, D. Mecerreyes, *J. Polym. Sci. Polym. Chem.* 48 (2010) 4648–4653.
- [20] L. Liang, J. Liu, C.F. Windisch, G.J. Exarhos, Y.H. Lin, *Angew. Chem. Int. Ed.* 41 (2002) 3665–3668.
- [21] N.R. Chiau, C.M. Lui, J.J. Guan, L.J. Lee, A.J. Epstein, *Nat. Nanotechnol.* 2 (2007) 354–357.
- [22] C. Debiemme-Chouvy, *Electrochem. Commun.* 11 (2009) 298–301.
- [23] J. Huang, K. Wang, Z. Wei, *J. Mater. Chem.* 20 (2010) 1117–1121.
- [24] R. Tena-Zaera, J. Elias, C. Lévy-Clément, I. Mora-Seró, Y. Luo, J. Bisquert, *Phys. Status Solidi A* 205 (2008) 2345–2350.
- [25] M. Shamsipur, S.H. Kazemi, M.F. Mousavi, *Biosens. Bioelectron.* 24 (2008) 104–110.
- [26] M. Lin, M.S. Cho, W.S. Choe, Y. Lee, *Biosens. Bioelectron.* 25 (2009) 28–33.
- [27] M. Lin, M.S. Cho, W.S. Choe, Y. Son, Y. Lee, *Electrochim. Acta* 54 (2009) 7012–7017.
- [28] J.W. Lee, F. Serna, C.E. Schmidt, *Langmuir* 22 (2006) 9816–9819.
- [29] C. Xu, P. Shin, L. Cao, D. Gao, *J. Phys. Chem. C* 114 (2010) 125–129.
- [30] T. Pauporté, D. Lincot, B. Viana, F. Pellé, *Appl. Phys. Lett.* 89 (2006) 233112.
- [31] R. Tena-Zaera, J. Elias, G. Wang, C. Lévy-Clément, *J. Phys. Chem. C* 111 (2007) 16706–16711.
- [32] A. Sun, Z. Li, T. Wei, Y. Li, P. Cui, *Sens. Actuators B* 142 (2009) 197–203.
- [33] L.T. Qu, G.Q. Shi, F.E. Chen, J.X. Zhang, *Macromolecules* 36 (2003) 1063–1067.
- [34] W. Geng, N. Li, X. Li, R. Wang, J. Tu, T. Zhang, *Sens. Actuators B* 125 (2007) 114–119.
- [35] G. Świdorski, S. Wojtulewski, M. Kalinowska, R. Świśłocka, W. Lewandowski, *J. Mol. Struct.* 993 (2011) 448–458.
- [36] T. Uğur, Ş. Yücel, E. Nusret, U. Yasemin, P. Kadir, Y. Atilla, *J. Electroanal. Chem.* 570 (2004) 6–12.
- [37] S. Ghosh, G.A. Bowmaker, R.P. Cooney, J.M. Seakins, *Synth. Met.* 95 (1998) 63–67.
- [38] M. Yousef Elahi, S.Z. Bathaie, S.H. Kazemi, M.F. Mousavi, *Anal. Biochem.* 411 (2011) 176–184.
- [39] J. Gong, L. Wang, X. Miao, L. Zhang, *Electrochem. Commun.* 12 (2010) 1658–1661.
- [40] J. Wang, B. Tian, J. Wang, J. Lu, C. Olsen, C. Yarnitzky, K. Olsen, D. Hammerstrom, W. Bennett, *Anal. Chim. Acta* 385 (1999) 429–435.
- [41] M. Heitzmann, C. Bucher, J.C. Moutet, E. Pereira, B.L. Rivas, G. Royal, E. Saint-Aman, *Electrochim. Acta* 52 (2007) 3082–3087.
- [42] M.A. Rahman, M.S. Won, Y.B. Shim, *Anal. Chem.* 75 (2003) 1123–1129.